FEMS Yeast Research, 21, 2021, foab033

https://doi.org/10.1093/femsyr/foab033
Advance Access Publication Date: 27 May 2021
Research Article

RESEARCH ARTICLE

Evolutionary engineering reveals amino acid substitutions in Ato2 and Ato3 that allow improved growth of *Saccharomyces cerevisiae* on lactic acid

Nicolò Baldi[1,†], Sophie Claire de Valk[1,†,‡], Maria Sousa-Silva[2,3,§], Margarida Casal[2,3], Isabel Soares-Silva[2,3,¶] and Robert Mans[1,*]

[1]Department of Biotechnology, Delft University of Technology, Van der Maasweg 9, 2629HZ Delft, The Netherlands, [2]Centre of Molecular and Environmental Biology (CBMA), University of Minho, Campus de Gualtar, 4710-057 Braga, Portugal and [3]Institute of Science and Innovation for Bio-Sustainability (IB-S), University of Minho, Campus de Gualtar, 4710-057 Braga, Portugal

*Corresponding author: Department of Biotechnology, Delft University of Technology, Van der Maasweg 9, 2629HZ Delft, The Netherlands. Tel: +31 15 27 84 630; E-mail: r.mans@tudelft.nl

One sentence summary: Identification and characterization of two transport proteins (Ato2 and Ato3) in *Saccharomyces cerevisiae* that facilitate lactic acid uptake after gaining specific point mutations during evolutionary engineering.

†Shared-first authorship.

Editor: John Morrissey

‡Sophie Claire de Valk, http://orcid.org/0000-0001-7314-9533
§Maria Sousa-Silva, http://orcid.org/0000-0003-1622-4888
¶Isabel Soares-Silva, http://orcid.org/0000-0001-8431-1567

ABSTRACT

In *Saccharomyces cerevisiae*, the complete set of proteins involved in transport of lactic acid across the cell membrane has not been determined. In this study, we aimed to identify transport proteins not previously described to be involved in lactic acid transport via a combination of directed evolution, whole-genome resequencing and reverse engineering. Evolution of a strain lacking all known lactic acid transporters on lactate led to the discovery of mutated Ato2 and Ato3 as two novel lactic acid transport proteins. When compared to previously identified *S. cerevisiae* genes involved in lactic acid transport, expression of $ATO3^{T284C}$ was able to facilitate the highest growth rate (0.15 ± 0.01 h^{-1}) on this carbon source. A comparison between (evolved) sequences and 3D models of the transport proteins showed that most of the identified mutations resulted in a widening of the narrowest hydrophobic constriction of the anion channel. We hypothesize that this observation, sometimes in combination with an increased binding affinity of lactic acid to the sites adjacent to this constriction, are responsible for the improved lactic acid transport in the evolved proteins.

Keywords: evolutionary engineering; transport; protein structure; reverse engineering; carboxylic acids

INTRODUCTION

The yeast *Saccharomyces cerevisiae* is able to utilize a variety of compounds as carbon and energy source, including monosaccharides, disaccharides, monocarboxylic acids, amino acids and polyols (Lagunas 1993; Kruckeberg and Dickinson 2004). Assimilation and dissimilation of these compounds inside cells is preceded by their transport across the plasma membrane. A lot of research has been dedicated to the identification of

Received: 30 November 2020; **Accepted:** 25 May 2021

proteins involved in uptake, and the elucidation of their structure, function and mechanism of action, both to understand cellular response to different conditions as well as for the application of metabolic engineering strategies to increase the efficiency of substrate usage and broaden the substrate range of industrial cell factories (Agrimi and Steiger 2021).

This research field has tremendously benefitted from engineered 'platform strains', in which all transporters for a certain substrate have been knocked out. One of the most applied platform strains is the so called '*hxt*^{0} strain', in which the uptake of hexoses is completely abolished by the knockout of all 21 genes involved in the uptake of hexoses (Wieczorke *et al.* 1999). This *hxt*^{0} strain has been indispensable for studies where both endogenous and heterologous proteins were characterized for their ability to catalyze the uptake of various hexose and pentose sugars (Anjos *et al.* 2013; Li *et al.* 2015; Gao, Ploessl and Shao 2019; Bueno *et al.* 2020; Chattopadhyay *et al.* 2020; Huang *et al.* 2020; Morii *et al.* 2020). The absence of all hexose transporters in this strain renders it unable to grow on media in which a monosaccharide is the sole carbon source, and therefore allows for screening of growth phenotypes that are linked to the expression of an investigated transport protein. The application of the *hxt*^{0} strain is also preferred for *in vivo* transport assays in which the intracellular accumulation of substrates is measured, since background signal caused by other transporters is minimized (Paulsen, Custódio and Pedersen 2019; Nogueira *et al.* 2020; Schmidl *et al.* 2021). In addition, it has often been used as background strain in directed evolution of (heterologous) transport proteins, for which selection is based on growth on the transported substrate (Wang *et al.* 2013; Colabardini *et al.* 2014; Zhang *et al.* 2015; Li, Schmitz and Alper 2016; Sloothaak *et al.* 2016; Nijland and Driessen 2020). The benefit of a platform strain in an evolutionary engineering approach is that the presence of other genes that could (upon mutation) provide a selective advantage is minimized, and thus allows for improved selection of mutants of the gene under investigation. Similar platform strains have been constructed to study disaccharide transporters (Riesmeier, Willmitzer and Frommer 1992) and ABC transporters (Suzuki *et al.* 2011).

Transport of monocarboxylic acids across the yeast plasma membrane remains enigmatic (Borodina 2019) and therefore the establishment of specialized platform strains to study transport of specific monocarboxylic acids could be an important next step to further our understanding. Whereas the undissociated, protonated form of carboxylic acids can cross biological membranes by passive diffusion, the charged anionic form that is predominant in pH conditions well above the pK_a of the acid requires (a) protein(s) to mediate rapid transport across the membrane (Gabba *et al.* 2020). These monocarboxylic acid transport proteins play an important role in, for instance, food preservation, weak organic acid tolerance in second generation bioethanol production, metabolic engineering strategies for industrial production of carboxylic acids and in development of cancer therapies (Pinheiro *et al.* 2012; Soares-Silva *et al.* 2020). Two genes encoding permeases for monocarboxylic acids have been identified so far in *S. cerevisiae*: *JEN1* and *ADY2* (Casal *et al.* 2016). Jen1 is a member of the Major Facilitator Superfamily which enables uptake of lactic, acetic and pyruvic acid (Casal *et al.* 1999). Ady2 is an acetate transporter that belongs to the AceTr family, for which two homologs have been described in *S. cerevisiae*, Ato2 and Ato3 (Paiva *et al.* 2004; Ribas *et al.* 2019). A powerful strategy to identify more genes involved in a specific physiological function is the use of adaptive laboratory evolution. Application of a selective pressure is used to enrich for mutants with the phenotype of interest, which can subsequently be analyzed by whole genome sequencing to identify mutated genes related to the evolved phenotype (Mans, Daran and Pronk 2018). This concept was demonstrated in a previous study, in which laboratory evolution of a *jen1*Δ strain in culture medium with lactic acid as sole carbon source led to the identification of mutated *ADY2* alleles that had an increased uptake capacity for lactic acid (de Kok *et al.* 2012). Lactic acid, which is produced on industrial scale using biotechnological processes, is used as preservative in the dairy industry and as a precursor for the production of bioplastic, with a demand of 1.220.000 tons in 2016 that is expected to further increase by 16.2% before 2025 (Singhvi, Zendo and Sonomoto 2018).

In this study, we use adaptive laboratory evolution to identify additional transporters, which upon mutation can efficiently catalyze lactic acid uptake in *S. cerevisiae*. Subsequently, we overexpress the complete suite of native and evolved lactic acid transporters in a strain background devoid of all (putative) organic acid transporters, characterize the ability of the resulting strains to grow on monocarboxylic acids and assess the uptake of labeled lactate and acetate by the evolved transporters. Finally, we identify specific amino acid residues playing a key role in the transport of lactic acid and provide a mechanistic explanation using three-dimensional structure predictions combined with molecular docking analysis.

MATERIALS AND METHODS

Strains and maintenance

The *S. cerevisiae* strains used in this study (Table 2) share the CEN.PK113-7D or the CEN.PK2-1C genetic backgrounds (Entian and Kötter 2007). Stock cultures of *S. cerevisiae* were grown aerobically in 500 mL round-bottom shake flasks containing 100 mL synthetic medium (SM; Verduyn *et al.* 1992) or YP medium (10 g/L Bacto yeast extract and 20 g/L Bacto peptone) supplemented with 20 g/L glucose. When needed, auxotrophic requirements were complemented via addition of 150 mg/L uracil, 100 mg/L histidine, 500 mg/L leucine and/or 75 mg/L tryptophan (Pronk 2002). For plate cultivation, 2% (w/v) agar was added to the medium prior to heat sterilization. Stock cultures of *E. coli* XL1-Blue Subcloning Grade Competent Cells (Agilent, Santa Clara, CA) that were used for plasmid propagation were grown in LB medium (5 g/L Bacto yeast extract, 10 g/L Bacto tryptone and 10 g/L NaCl) supplemented with 100 mg/L ampicillin. Media were autoclaved at 121°C for 20 min and supplements and antibiotics were filter sterilized and added to the media prior to use. Frozen culture stocks were prepared by addition of sterile glycerol (to a final concentration of 30% v/v) to exponentially growing shake flask cultures of *S. cerevisiae* or overnight cultures of *E. coli* and 1 mL aliquots were stored at −80°C.

Molecular biology techniques

Phusion High-Fidelity DNA Polymerase (Thermo Fisher Scientific, Waltham, MA) was used for PCR amplification for cloning purposes. Diagnostic PCRs were performed using DreamTaq PCR Master Mix (2X; Thermo Fisher Scientific). In both cases, the manufacturer's protocol was followed, with the exception of the use of lower primer concentrations (0.2 μM each). Desalted (DST) oligonucleotide primers were used, except for primers binding to coding regions, which were PAGE purified. Primers were purchased from Sigma Aldrich (Saint Louis, MO), with the exception of primers 17452 and 17453, which

Table 1. Plasmids used in this study.

Name	Relevant characteristic	Origin
pROS13	2μm ampR kanMX gRNA-CAN1 gRNA-ADE2	Mans *et al.* (2015)
pROS10	2μm ampR URA3 gRNA-CAN1 gRNA-ADE2	Mans *et al.* (2015)
pMEL13	2μm ampR kanMX gRNA-CAN1	Mans *et al.* (2015)
pUDR405	2μm ampR *kan*MX gRNA-JEN1 gRNA-ADY2	This study
pUDR420	*2μm ampR* kanMX *gRNA-ATO3*	This study
pUDR767	2μm ampR URA3 gRNA-ATO2	This study
p426-TEF	2μm *URA3 pTEF1-tCYC1*	Mumberg *et al.* (1995)
pUDE813	2μm *URA3 pTEF1-ATO3-tCYC1*	This study
pUDE814	*2μm URA3 pTEF1-ATO3*^{T284C}*-tCYC1*	This study
pUDE1001	2μm *URA3 pTEF1-JEN1-tCYC1*	This study
pUDE1002	2μm *URA3 pTEF1-ADY2-tCYC1*	This study
pUDE1003	*2μm URA3 pTEF1- ADY2*^{C755G} *-tCYC1*	This study
pUDE1004	*2μm URA3 pTEF1- ADY2*^{C655G}*-tCYC1*	This study
pUDE1021	2μm *URA3 pTEF1-ATO2-tCYC1*	This study
pUDE1022	*2μm URA3 pTEF1-ATO2*^{T653C}*-tCYC1*	This study
pUDC156	*CEN6 URA3 pTEF-CAS9-tCYC1*	Marques *et al.* (2017)
pUDC319	*CEN6 URA3 pTEF-tCYC1*	This study
pUDC320	*CEN6 URA3 pTEF1-ATO3-tCYC1*	This study
pUDC321	*CEN6 URA3 pTEF1-ATO3*^{T284C}*-tCYC1*	This study
pUDC322	*CEN6 URA3 pTEF1-JEN1-tCYC1*	This study
pUDC323	*CEN6 URA3 pTEF1-ADY2-tCYC1*	This study
pUDC324	*CEN6 URA3 pTEF1- ADY2*^{C755G} *-tCYC1*	This study
pUDC325	*CEN6 URA3 pTEF1- ADY2*^{C655G}*-tCYC1*	This study
pUDC326	*CEN6 URA3 pTEF1-ATO2-tCYC1*	This study
pUDC327	*CEN6 URA3 pTEF1-ATO2*^{T653C}*-tCYC1*	This study

were purchased from Ella Biotech (Planegg, Germany). For diagnostic PCR, yeast genomic DNA was isolated as described by Lõoke, Kristjuhan and Kristjuhan (2011). Commercial kits for DNA extraction and purification were used for small-scale DNA isolation (Sigma Aldrich), PCR cleanup (Sigma Aldrich) and gel extraction (Zymo Research, Irvine, CA). Restriction analysis of constructed plasmids was performed using FastDigest restriction enzymes (Thermo Scientific). Gibson assembly of linear DNA fragments was performed using NEBuilder HiFi DNA Assembly Master Mix (New England Biolabs, Ipswich, MA) in a total reaction volume of 5 μL. Transformation of chemically competent *E. coli* XL1-Blue (Agilent) was performed according to the manufacturer's protocol.

Plasmid construction

The plasmids and oligonucleotide primers used in this study are listed in Table 1 and Table S1 (Supporting Information), respectively. All plasmids were constructed by Gibson assembly of two linear fragments. With the exception of the fragments used for the construction of plasmid pUDR420, all fragments were PCR-amplified from either a template plasmid or from genomic DNA.

Plasmid pUDR405 was constructed by Gibson assembly of two linear fragments, both obtained via PCR amplification of plasmid pROS13 using primers 8664 and 6262 (for the *JEN1*-gRNA_2μ_*ADY2*-gRNA insert) and 6005 (for the plasmid backbone), as previously described by (Mans *et al.* 2015). Plasmid pUDR420 was constructed by Gibson assembly of a double-stranded DNA fragment, obtained by annealing the complementary single-stranded oligonucleotides 8691 and 13552, and a vector backbone amplified from plasmid pMEL13 using primers 6005 and 6006. Plasmid pUDR767 was constructed by Gibson assembly of two linear fragments, both obtained via PCR amplification of plasmid pROS10 using primers 8688 (for the *ATO2*-gRNA_2μ_*ATO2*-gRNA insert) and 6005 (for the plasmid backbone). For construction of pUDE813, the linear p426-TEF plasmid backbone was amplified from plasmid p426-TEF using primers 5921 and 10547 and the *ATO3* open reading frame (ORF) was amplified from yeast strain CEN.PK113-7D genomic DNA using primers 13513 and 13514. Subsequently, Gibson assembly of the linear p426-TEF plasmid backbone and the *ATO3* insert yielded pUDE813. pUDE814, pUDE1001, pUDE1002, pUDE1003, pUDE1004, pUDE1021 and pUDE1022 were constructed similar to pUDE813, using primers 5921 and 10547 to amplify the linear p426-TEF plasmid backbone. The inserts were amplified from genomic DNA of strain CEN.PK113-7D (for wildtype genes) or from genomic DNA of the corresponding evolved strain (for mutated genes) using primers 13513 and 13514 (pUDE814), 17170 and 17171 (pUDE1001), 17168 and 17169 (pUDE1002, pUDE1003 and pUDE1004) or 17452 and 17453 (pUDE1021 and pUDE1022). For construction of pUDC319, plasmid p426-TEF was amplified using primers 2949 and 17741 and the CEN6 origin of replication was amplified from pUDC156 using primers 17742 and 17743. Subsequently, Gibson assembly of the linear p426-TEF plasmid fragment and the CEN6 fragment yielded pUDC319. pUDC320, pUDC321, pUDC322, pUDC323, pUDC324, pUDC325, pUDC326 and pUDC327 were constructed in a similar way using the same primers, but the linear plasmid fragment was amplified from pUDE813, pUDE814, pUDE1001, pUDE1002, pUDE1003, pUDE1004, pUDE1021 and pUDE1022, respectively.

Strain construction

Saccharomyces cerevisiae strains were transformed with the LiAc/ssDNA method (Gietz and Woods 2002). For transformations with a dominant marker, the transformation mixture was plated on YP plates, containing glucose (20 g/L) as carbon source, and supplemented with 200 mg/L G418 (Invitrogen, Carlsbad, CA). Gene deletions were performed as previously described (Mans *et al.* 2015). For transformation of plasmids harboring

Table 2. *Saccharomyces cerevisiae* strains used in this study.

Strain name	Relevant genotype	Origin
CEN.PK113-7D	Prototrophic reference, *MATa*	Entian and Kötter (2007)
IMX581	*MATa ura3-52 can1::cas9-natNT2*	Mans *et al.* (2015)
IMX585	*MATa can1::cas9-natNT2*	Mans *et al.* (2015)
IMK341	*MATa ura3::loxP ady2::loxP-hphNT1-loxP jen1::loxP*	de Kok *et al.* (2012)
IMW004	*MATa URA3 ADY2*^{C755G} *jen1::loxP-KanMX4-loxP*	de Kok *et al.* (2012)
IMW005	*MATa URA3 ADY2*^{C655G} *jen1::loxP-KanMX4-loxP*	de Kok et al. (2012)
IMX1000	*MATa ura3-52 trp1-289 leu2-3112 his3Δ can1Δ::cas9-natNT2 mch1Δ mch2Δ mch5Δ aqy1Δ itr1Δ pdr12Δ mch3Δ mch4Δ yil166cΔ hxt1Δ jen1Δ ady2Δ aqr1Δ thi73Δ fps1Δ aqy2Δ yll053cΔ ato2Δ ato3Δ aqy3Δ tpo2Δ yro2Δ azr1Δ yhl008cΔ tpo3Δ*	Mans *et al.* (2017)
IMK875	*MATa can1::cas9-natNT2 jen1Δ ady2Δ*	This study
IMK876	*MATa can1::cas9-natNT2 ura3-52 jen1Δ ady2Δ*	This study
IMK882	*MATa can1::cas9-natNT2 jen1Δ ady2Δ ato3Δ*	This study
IMK883	*MATa can1::cas9-natNT2 ura3-52 jen1Δ ady2Δ ato3Δ*	This study
IMK982	*MATa can1::cas9-natNT2 ura3-52 jen1Δ ady2Δ ato3Δ ato2Δ*	This study
IMS807	IMK341 evolved for growth on lactate, evolution line A	This study
IMS808	IMK341 evolved for growth on lactate, evolution line A	This study
IMS809	IMK341 evolved for growth on lactate, evolution line A	This study
IMS810	IMK341 evolved for growth on lactate, evolution line B	This study
IMS811	IMK341 evolved for growth on lactate, evolution line B	This study
IMS1122	IMK882 evolved for growth on lactate	This study
IMS1123	IMK882 evolved for growth on lactate	This study
IMS1130	IMK882 evolved for growth on lactate	This study
IMX2486	IMX1000 *ura3-52 TRP1, leu2-3112, his3Δ*	This study
IMX2487	IMX1000 *ura3-52 TRP1, LEU2, his3Δ*	This study
IMX2488	IMX1000 *ura3-52 TRP1, LEU2, HIS3*	This study
IME581	IMX2488 p426-TEF (2μm)	This study
IME582	IMX2488 pUDE813 (2μm *ATO3*)	This study
IME583	IMX2488 pUDE814 (2μm *ATO3*^{T284C})	This study
IME584	IMX2488 pUDE1001 (2μm *JEN1*)	This study
IME585	IMX2488 pUDE1002 (2μm *ADY2*)	This study
IME586	IMX2488 pUDE1003 (2μm *ADY2*^{C755G})	This study
IME587	IMX2488 pUDE1004 (2μm *ADY2*^{C655G})	This study
IME588	IMX2488 pUDE1021 (2μm *ATO2*)	This study
IME589	IMX2488 pUDE1022 (2μm *ATO2*^{T653C})	This study
IMC164	IMX2488 pUDC319 (*CEN6*)	This study
IMC165	IMX2488 pUDC320 (*CEN6 ATO3*)	This study
IMC166	IMX2488 pUDC321 (*CEN6 ATO3*^{T284C})	This study
IMC167	IMX2488 pUDC322 (*CEN6 JEN1*)	This study
IMC168	IMX2488 pUDC323 (*CEN6 ADY2*)	This study
IMC169	IMX2488 pUDC324 (*CEN6 ADY2*^{C755G})	This study
IMC170	IMX2488 pUDC325 (*CEN6 ADY2*^{C655G})	This study
IMC171	IMX2488 pUDC326 (*CEN6 ATO2*)	This study
IMC172	IMX2488 pUDC327 (*CEN6 ATO2*^{T653C})	This study

Table 3. Amino acid changes identified by whole-genome sequencing of single colony isolates evolved for growth in medium containing lactic acid as sole carbon source. Isolates IMS807–IMS811 are derived from IMK341 (*jen1*Δ and *ady2*Δ) and IMS1122 and IMS1123 are derived from IMK882 (*jen1*Δ, *ady2*Δ and *ato3*Δ). IMS807, IM808 and IMS809 are isolates from evolution line #1 and IMS810 and IMS811 are isolates from evolution line #2. The mutation Sip5^{*490Q} indicates loss of the stop codon.

IMK341 evolution #1			IMK341 evolution #2		IMK822 evolution #1	IMK822 evolution #2
IMS807	IMS808	IMS809	IMS810	IMS811	IMS1122	IMS1123
Ato3^{F95S}	**Ato3**^{F95S}	**Ato3**^{F95S}	**Ato3**^{F95S}	**Ato3**^{F95S}	**Ato2**^{L218S}	**Ato2**^{L218S}
Mms2^{Y58C}	Mms2^{Y58C}	Mms2^{Y58C}	Sip5^{*490Q}	Sip5^{*490Q}	Lrg1^{H979N}	Whi2^{E119*}
Pih1^{D147Y}	Pih1^{D147Y}	Pih1^{D147Y}	Ssn2^{M1280R}	Lip5^{R4L}	Ykr051w^{Y285H}	Ykr051w^{Y285H}
Uba1^{L952F}		Drn1^{P213L}			Jjj1^{H356Q}	Jjj1^{H356Q}
Stv1^{L275F}					Trm10^{A49V}	Trm10^{A49V}
Whi2^{E187*}						
Vba4^{P198L}						

an auxotrophic marker, transformed cells were plated on SM medium with glucose (20 g/L) as a carbon source and when needed, appropriate auxotrophic requirements were supplemented.

The tryptophan auxotrophy of IMX1000 was the result of a single point mutation in the *TRP1* gene (*trp1-289*; Botstein *et al.* 1979) and was spontaneously reverted by plating the strain on SM medium supplemented with uracil, histidine and leucine, and picking a tryptophan prototrophic colony, yielding strain IMX2486. Strain IMX2487 was constructed by transforming IMX2486 with a linear fragment, obtained by PCR amplification of the *LEU2* gene from CEN.PK113-7D, using primers 1742 and 1743. Strain IMX2488 was constructed by transforming IMX2487 with a linear fragment, obtained by PCR amplification of the *HIS3* gene from CEN.PK113-7D, using primers 1738 and 3755. Strain IMK875 was constructed by transforming the Cas9-expressing strain IMX585 with plasmid pUDR405 and two double stranded repair oligonucleotides obtained by annealing oligonucleotides 8597–8598 and 8665–8666. Strain IMK876 was constructed by transforming the Cas9-expressing strain IMX581 with plasmid pUDR405 and two double strained repair oligonucleotides obtained by annealing oligonucleotides 8597–8598 and 8665–8666. Strains IMK882 and IMK883 were obtained by transforming strains IMK875 and IMK876, respectively, with plasmid pUDR420 and a double stranded repair oligonucleotide obtained by annealing oligonucleotides 14120 and 14121. Strain IMK982 was constructed by transforming strain IMK883 with plasmid pUDR767 and a double stranded repair oligonucleotide obtained by annealing oligonucleotides 8689 and 8690. Plasmids p426-TEF, pUDE813, pUDE814, pUDE1001, pUDE1002, pUDE1003, pUDE1004, pUDE1021, pUDE1022, pUDC319, pUDC320, pUDC321, pUDC322, pUDC323, pUDC324, pUDC325, pUDC326 and pUDC327 were transformed in strain IMX2488, yielding IME581, IME582, IME583, IME584, IME585, IME586, IME587, IME588, IME589, IMC164, IMC165, IMC166, IMC167, IMC168, IMC169, IMC170, IMC171 and IMC172, respectively.

Evolution of IMK341 and IMK882 was performed by inoculating duplicate shake flasks with 20 mL synthetic medium with lactic acid as the sole carbon source (SML, see Section 2.5 'Media and cultivation') with these strains to obtain a starting optical density (OD) of 0.1. Once the cultures grew and stationary phase was reached, a 1 mL aliquot of each culture was transferred to 20 mL fresh SML and grown until stationary phase again (in total approximately 14 generations for IMK341 and 7 generations for IMK882). Single colony isolates from these evolution cultures ('IMS'-strains) were obtained by plating the cultures using an inoculation loop (~10 μL) on solid SML and restreaking a grown colony to a fresh plate three consecutive times, after which one colony was grown in liquid SML and stocked.

Media and cultivation

Evolution experiments were performed in 500 mL shake-flask cultures containing 100 mL synthetic medium (Verduyn *et al.* 1992) with 84 mM L-lactic acid as sole carbon source. The pH of the medium was set at 5.0 and the cultures were incubated at 30°C in an Innova incubator shaker (New Brunswick Scientific, Edison, NJ) set at 200 rpm. Auxotrophic requirements were supplemented as needed.

Strains were characterized in SM supplemented with different carbon sources. To achieve an initial carbon concentration of 250 mM, the culture media contained either 42 mM D-glucose, 83 mM L-lactic acid, 125 mM acetic acid or 83 mM pyruvic acid. The characterization was performed in a Growth-Profiler system (EnzyScreen, Heemstede, The Netherlands) equipped with 96-well plates in a culture volume of 250 μL, set at 250 rpm and 30°C. The measurement interval was set at 30 min. Raw green values were corrected for well-to-well variation using measurements of a 96-well plate containing a culture with an externally determined optical density of 3.75 in all wells. Optical densities were calculated by converting green values (corrected for well-to-well variation) using a calibration curve that was determined by fitting a third-degree polynomial through 22 measurements of cultures with known OD values between 0.1 and 20. Growth rates were calculated using the calculated optical densities of at least 15 points in the exponential phase. Exponential growth was assumed when an exponential curve could be fitted with an R^2 of at least 0.985.

Analytical methods

Culture optical density at 660 nm was measured with a Libra S11 spectrophotometer (Biochrom, Cambridge, United Kingdom). In order to measure within the linear range of the instrument (OD between 0.1 and 0.3), cultures were diluted in an appropriate amount of demineralized water. Metabolite concentrations in culture supernatants and media were analyzed using an Agilent 1260 Infinity HPLC system equipped with a Bio-rad Aminex HPX-87H ion exchange column, operated at 60°C with 5 mM H_2SO_4 as mobile phase at a flow rate of 0.600 mL/min.

DNA extraction and whole genome sequencing

Strain IMK341 and the evolved single colony isolates (IMS-strains) were grown in 500 mL shake flasks containing 100 mL YP medium supplemented with glucose (20 g/L) as a carbon source. The cultures were incubated at 30°C until the strains reached stationary phase and genomic DNA was isolated using the Qiagen 100/G kit (Qiagen, Hilden, Germany) according to the manufacturer's instructions and quantified using a Qubit® Fluorometer 2.0 (Thermo Fisher Scientific). The isolated DNA was sequenced in-house on a MiSeq (Illumina, San Diego, CA) with 300 bp paired-end reads using TruSeq PCR-free library preparation (Illumina). For all the strains, the reads were mapped onto the *S. cerevisiae* CEN.PK113-7D genome (Salazar *et al.* 2017) using the Burrows–Wheeler Alignment tool (BWA) and further processed using SAMtools and Pilon for variant calling (Li *et al.* 2009; Li and Durbin 2010; Walker *et al.* 2014).

Transport assays

The uptake of labeled carboxylic acids was assessed as previously described by Ribas *et al.* (2017), using [1–^{14}C] acetic acid (Perkin Elmer, Waltham, MA) and [U-^{14}C] L-lactic acid (Perkin Helmer) with a specific activity of 2000 dpm/nmol. The data shown are mean values of at least three independent experiments.

3D modeling and molecular docking of Ady2, Ato2 and Ato3

The three-dimensional modeling analysis was performed for the protein sequences of Ato1, Ady2^{L219V}, Ady2^{A252G}, Ato2, Ato2^{L218S}, Ato3 and Ato3^{F95S}. The amino acid sequences were retrieved from the *Saccharomyces* Genome Database (Cherry *et al.* 2012). To determine the predicted transporter 3D structures, the amino acid sequences were threaded through the PDB library using

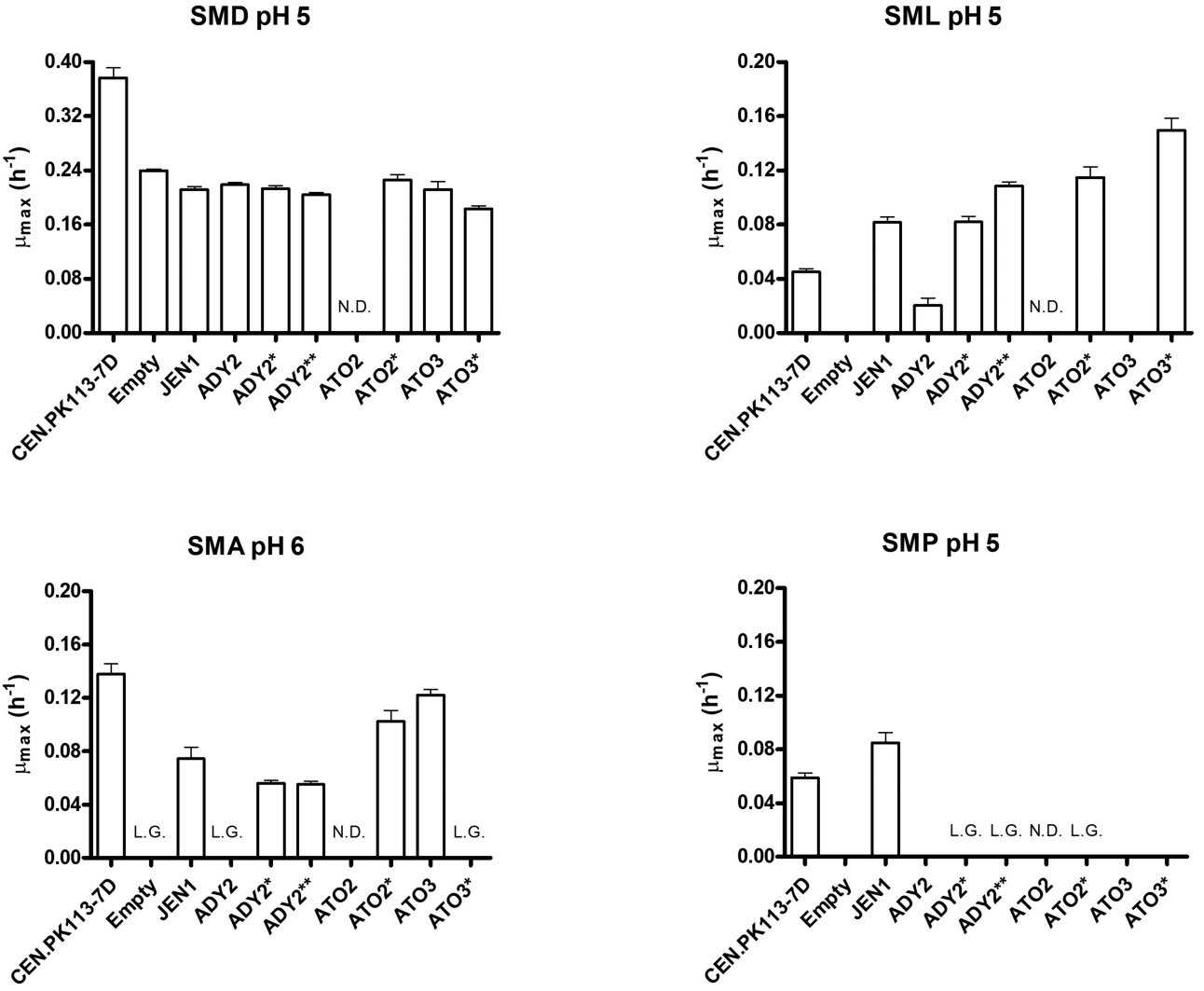

Figure 1. Growth rates on different sole carbon sources of *S. cerevisiae* reference strain CEN.PK113-7D and the 25-transporter deletion strain IMX2488 expressing an empty vector or a vector carrying the indicated organic acid transporter. Bars and error bars represent the average and standard deviation of three independent experiments. SMD: synthetic medium with 42 mM glucose. SML: synthetic medium with 83 mM lactic acid. SMA: synthetic medium with 125 mM acetic acid. SMP: synthetic medium with 83 mM pyruvic acid. Empty: empty plasmid. ADY2*: ADY2^{C755G} allele. ADY2**: ADY2^{C655G} allele. ATO2*: ATO2^{T653C} allele. ATO3*: ATO3^{T284C} allele. For some experiments, a linear increase in optical density was observed, which impeded the determination of an exponential growth rate (indicated by L.G. for Linear Growth). N.D.: not determined.

LOMETS (Local Meta-Threading-Server). The *Citrobacter koseri* succinate acetate permease (CkSatP and PDB 5YS3) was the top ranked template threading identified in LOMETS for Ato1, Ato2 and Ato3 (Qui *et al.* 2018). Since the CkSatP three-dimensional modeling obtained the best score for protein structure prediction, it was further considered for molecular docking analysis. CkSatP presents a protein identity of 35% with Ady2, 34% with Ato2 and 28% with Ato3 and similarity of 0.566, 0.548 and 0.515, respectively. Molecular docking simulations were performed as described by Ribas *et al.* (2017). Ligand structures of acetic, lactic and pyruvic acid for all target proteins in the study were downloaded from the Zinc database (Sterling and Irwin 2015). Structures used for docking were all confirmed in Maestro v11.2 before ligand-protein simulations were performed using AutoDock Vina in the PyRx software (Trott and Olson 2010). The docking studies were performed with the dissociated forms of each carboxylic acid. The protonation states were adjusted to match a pH of 5.0–6.0 and exported in the mol2 format. Docking was performed with four docking-boxes for each protein, containing top, bottom and middle-structure parts for a more robust use of Autodock Vina program. The exhaustiveness parameter was set up for 1000 calculations for each of the grid-zones defined for docking. The generated docking scores and 2–3D pose views were evaluated for the establishment of molecular interactions and ligand binding affinities.

RESULTS

Laboratory evolution on lactic acid leads to point mutations in Ato2 or Ato3

In an attempt to identify additional transporters able to catalyze the uptake of lactic acid after gaining point mutations, we incubated strains IMK341 and IMX1000 in duplicate shake flasks cultures containing synthetic medium with lactic acid as the sole carbon source. In IMK341 the known carboxylic acid transporters *JEN1* and *ADY2* are knocked out (*jen1*Δ, *ady2*Δ), whereas IMX1000 contains a further 23 deletions in putative

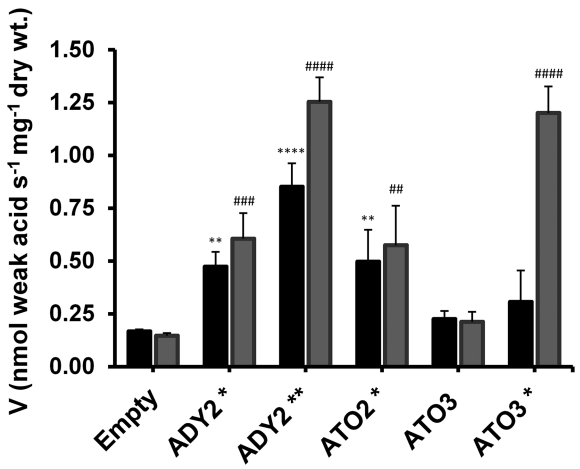

Figure 2. Transport of acetate and lactate in *S. cerevisiae* IMX1000 cells expressing native and evolved *ADY2*, *ATO2* and *ATO3*. Black bars: uptake of 5 mM of ^{14}C-acetic acid (pH 6.0). Grey bars: uptake of ^{14}C-lactic acid (pH 5.0). Empty: empty plasmid. ADY2*: $ADY2^{C755G}$ allele. ADY2**: $ADY2^{C655G}$ allele. ATO2*: $ATO2^{T653C}$ allele. ATO3*: $ATO3^{T284C}$ allele. Cells were grown on YNB-glucose, washed and incubated in YNB-lactate (0.5%, pH 5.0) for 4 h at 30°C. Statistical significance was estimated by one-way ANOVA followed by a post hoc Tukey's multiple comparisons test as follows: ** $P < 0.01$, *** $P < 0.001$ and **** $P < 0.0001$, acetate uptake significantly different from cells transformed with empty plasmid; ## $P < 0.01$, ### $P < 0.001$ and #### $P < 0.0001$, lactate uptake significantly different from cells transformed with empty plasmid.

lactic acid transporter-encoding genes (Table 2; Mans *et al.* 2017). After 9 weeks, growth was observed in both cultures of IMK341 whereas no growth was observed after 12 weeks of incubation of IMX1000. Whole-genome sequencing of evolved IMK341 (*jen1*Δ and *ady2*Δ) cell lines, named IMS807-811, which were isolated after a transfer to fresh medium, revealed three to seven non-synonymous SNPs in each mutant and no chromosomal duplications or rearrangements (Table 3). Strikingly, all evolved isolates shared an identical mutation in *ATO3* ($ATO3^{T284C}$). To investigate the role of *ATO3* in lactic acid uptake, we overexpressed both the native and evolved *ATO3* in IMK883 (*jen1*Δ, *ady2*Δ and *ato3*Δ) and tested the resulting strains for growth on SM lactic acid plates. After 5 days, only the reference strain CEN.PK113-7D and the strain carrying the $ATO3^{T284C}$ allele were able to grow (Figure S1, Supporting Information), indicating that the T284C mutation in *ATO3* was responsible for the evolved phenotype. We then combined the deletion of *JEN1*, *ADY2* and *ATO3* in strain IMK882 (*jen1*Δ, *ady2*Δ and *ato3*Δ) and repeated the evolution. After 5 and 12 days, growth was observed in two independent cultures from which evolved strains IMS1122 and IMS1123 were isolated after transfer to a flask with fresh medium. In both single colony isolates, five SNPs were present (Table 3), including a common mutation in *ATO2*, ($ATO2^{T653C}$), which has also been described as an ammonium transporter together with *ATO3* and *ADY2* (Palková *et al.* 2002). Finally, the evolution was repeated with IMK982 (*jen1*Δ, *ady2*Δ, *ato3*Δ and *ato2*Δ), but no growth was observed after 12 weeks of incubation.

Overexpression of mutated transporters enables rapid growth in liquid medium with lactic acid as sole carbon source

Strikingly, the evolved transporters able to catalyze the uptake of lactic acid (*ATO2* and *ATO3* in this study, and *ADY2* in work by de Kok *et al.* 2012) represent all members of the *S. cerevisiae* Acetate Uptake Transporter Family (TCDB 2.A.96). To characterize the impact of the mutations on the transport of organic acids, cellular growth was evaluated in strains individually expressing *JEN1*, *ADY2*, *ATO2* and *ATO3* and their mutated alleles under control of the strong *TEF1* promotor (Mumberg, Müller and Funk 1995), via centromeric vectors in IMX2488, a strain background in which 25 (putative) organic acid transporters were deleted (Table 2). No viable cultures could be obtained with strains overexpressing wildtype *ATO2*, which suggests a severe toxic effect of the overexpression of *ATO2* on cellular physiology, and for this reason no growth rate could be reported. All other IMX2488-derived transporter expressing strains had similar growth rates in liquid medium with 42 mM glucose as carbon source compared to the empty vector control (IMC164), indicating no major physiological effects caused by the overexpression of the transporters when grown on glucose (Fig. 1, top left panel). Overexpression of the transporter variants from multicopy vectors resulted in a growth rate reduction of up to 66% compared to the empty vector reference when grown on glucose and were therefore not tested further (Figure S2, Supporting Information). In accordance with previous research, strains overexpressing *ADY2*, $ADY2^{C755G}$ and $ADY2^{C655G}$ showed a maximum specific growth rate of 0.02 ± 0.01 h^{-1}, 0.08 ± 0.01 h^{-1} and 0.10 ± 0.01 h^{-1} when grown in medium containing 83 mM lactic acid as carbon source, respectively (de Kok *et al.* 2012). Surprisingly, strains expressing the evolved $ATO2^{T653C}$ and $ATO3^{T284C}$ alleles outperformed all the other tested strains, with maximum specific growth rates of 0.11 ± 0.01 h^{-1} and 0.15 ± 0.01 h^{-1}, respectively (Fig. 1, top right panel and Figure S5, Supporting Information). These represent the highest reported growth rates reported for *S. cerevisiae* on this carbon source and indicate that, similar to the role of evolved Ato3 in IMS807-811, the mutations in Ato2 are responsible for the evolved phenotypes observed in IMS1122 and IMS1123 (Table 3). The transport of labeled lactic acid in strains expressing native *ATO3* and evolved *ADY2*, *ATO2* and *ATO3* is in accordance with the observed growth phenotypes (Fig. 2). An increased uptake rate was observed for all strains overexpressing evolved transporters compared to the empty vector control strain, whereas expression of wildtype *ATO3* did not lead to a significant alteration in lactic acid uptake (Fig. 2).

Mutations in *ATO2* and *ATO3* alter the uptake capacity for acetate and pyruvate

After demonstrating that the point mutations increased the catalytic activity of Ato2, Ato3 and Ady2 for lactic acid transport, we also investigated their ability to transport acetic and pyruvic acid (Fig. 1, bottom panels and Figures S6 and S7, Supporting Information). In liquid medium at pH 5.0 with 125 mM acetic acid (pK_a of 4.75), no growth was observed for any of the strains with the 25-deletion background, likely caused by acetic acid toxicity due to the absence of essential acetic acid exporters (Figure S3, Supporting Information). However, at pH 6.0 different growth characteristics were observed. The empty vector control strain exhibited slow non-exponential growth, which was also observed for the strains expressing native *ADY2* and the evolved *ATO3* variant. On the other hand, expression of native *ATO3* and the evolved *ADY2* and *ATO2* variants improved growth performance on medium with acetic acid as sole carbon source. With the exception of native *ATO3*, these results are in accordance with improved uptake rates observed in these strains, determined with labeled acetate (Fig. 2). In medium containing 83 mM pyruvic acid, no exponential growth was

```
                                                                                1stTMS
tr|A8ALU5|A8ALU5_CITK8  ----------------------------------MGNTKLANPAPLGLMGFGMTTILLN 25
sp|P25613|ADY2_YEAST    GDNNEYIYIGRQKFLKSDLYQAFGG--TLNPGLAPAPVHKFANPAPLGLSAFALTTFVLS 106
sp|P32907|ATO2_YEAST    GKNNEYIYIGRQKFLRDDLFEAFGG--TLNPGLAPAPVHKFANPAPLGLSGFALTTFVLS 105
sp|Q12359|ATO3_YEAST    YSDRDFITLGSSTYRRRDLLNALDRGDGEEGNCAKYTPHQFANPVPLGLASFSLSCLVLS 103  F95S
                                                          ::***.**** .*.:: ::*.
                                2ndTMS                                3rdTMS
tr|A8ALU5|A8ALU5_CITK8  LHNAGF--FALDGIILAMGIFYGGIAQIFAGLLEYKKGNTFGLTAFTSYGSFWLTLVAIL 83
sp|P25613|ADY2_YEAST    MFNARAQGITVPNVVVGCAMFYGGLVQLIAGIWEIALENTFGGTALCSYGGFWLSFAAIY 166
sp|P32907|ATO2_YEAST    MFNARAQGITIPNVVVGCAMFYGGLVQLIAGIWEIALENTFGGTALCSFGGFWLSFGAIY 165
sp|Q12359|ATO3_YEAST    LINANVRGVTDGKWALSLFMFFGGAIELFAGLLCFVIGDTYAMTVFSSFGGFWICYGYGL 163
                        : **    .:     :.  :*:**  :::**:      :*:. *.: *:*.**:
                                          4thTMS                        5thTMS
tr|A8ALU5|A8ALU5_CITK8  LMPKMGLTE------APNAQFLGAYLGLWGVFTLFMFFGTLKAARALQFVFLSLTVLFAL 137
sp|P25613|ADY2_YEAST    -IPWFGILEAYEDNESDLNNALGFYLLGWAIFTFGLTVCTMKSTVMFFLLFFLLALTFLL 225  L219V
sp|P32907|ATO2_YEAST    -IPWFGILDAYKDKESDLGNALGFYLLGWALFTFGLSVCTMKSTIMFFALFFLLAVTFLL 224  L218S
sp|Q12359|ATO3_YEAST    -TDTDNLVSGYTD-PTMLNNVIGFFLAGWTVFTFLMLMCTLKSTWGLFLLLTFLDLTFLL 221
                             .: .     :   : :* :*  * :**: : . *:*::  :  ::  * : * *
                                    6thTMS
tr|A8ALU5|A8ALU5_CITK8  LAFGNIAGNEAVIHVAGWIGLVCGASAIYLAMGEVLNEQFGRTI-----LPIGEAH--  188
sp|P25613|ADY2_YEAST    LSIGHFANRLGVTRAGGVLGVVVAFIAWYNAYAGVATKQNSYVLARPFPLPSTERVIF  283  A252G
sp|P32907|ATO2_YEAST    LSIANFTGEVGVTRAGGVLGVIVAFIAWYNAYAGIATRQNSYIMVHPFALPSNDKVFF  282
sp|Q12359|ATO3_YEAST    LCIGTFIDNNNLKMAGGYFGILSSCCGWYSLYCSVVSPSNSYLAFRAHTMPNAP----  275
                        *.:. : ..  :  ..* :*:: .  . *     : . . .       :*
```

Figure 3. Multiple sequence alignment of *Citrobacter koseri* SatP and *Saccharomyces cerevisiae* Ady2, Ato2 and Ato3. The multiple sequence alignment was built with ClustalOmega (https://www.ebi.ac.uk/Tools/msa/clustalo/). Localization of transmembrane segments (TMSs) was predicted with PSI/TM-Coffee (http://tcoffee.crg.cat/apps/tcoffee/do:tmcoffee). Blue rectangles indicate residues of the narrowest constriction site F98-Y155-L219 (amino acid numbers refer to Ady2; Qui *et al.* 2018). Bold, underlined letters indicate the mutated residue.

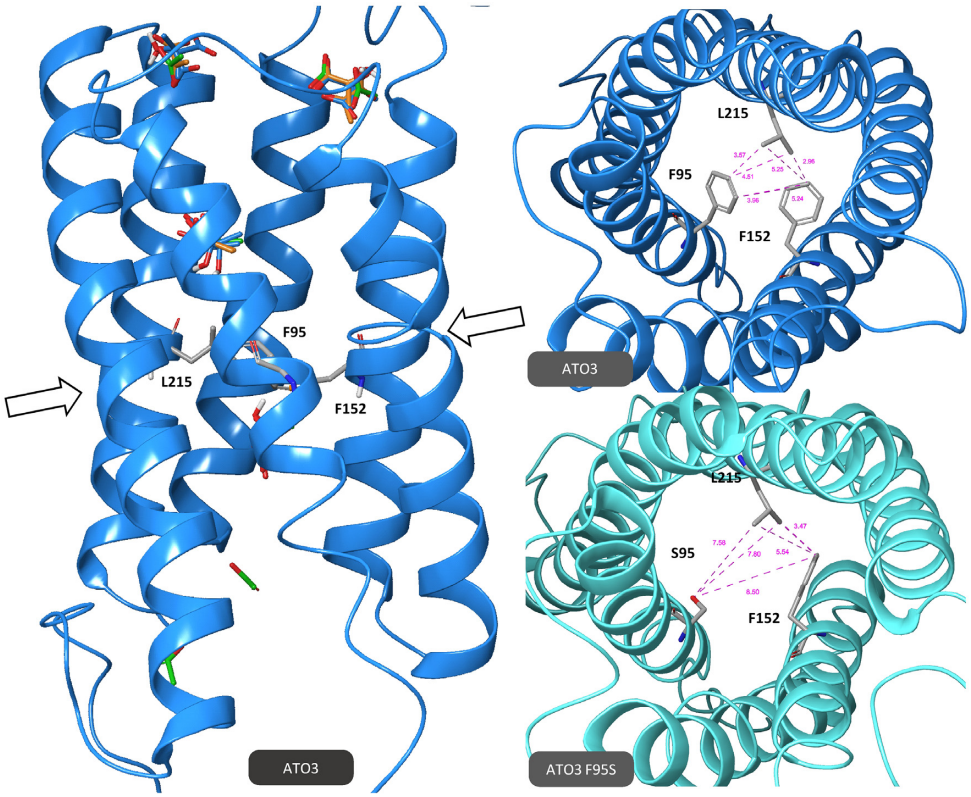

Figure 4. 3D models of the transporters Ato3 (dark blue) and Ato3^{F95S} (light blue). Left: side view of Ato3. Arrows indicate the hydrophobic constriction site, consisting of F95, L215 and F152. Binding sites for acetate (green ligand), lactate (blue ligand) and pyruvate (orange ligand) are presented. Right, top view of Ato3 (top) and Ato3^{F95S}(bottom). The amino acids involved in the constriction site are shown. Purple lines and values indicate estimated distances (in Å) between different anchor points of amino acids, calculated from the modeled protein structure.

Table 4. Estimated average distances (in Å) between different amino acids (AA) in the constriction pore of Ady2, Ato2, Ato3 and mutated alleles, calculated using the corresponding protein model. Bold values in the table indicate distances which are at least 1 Å larger than calculated in the reference structure.

	Estimated distance between AA residues			Protein	Estimated distance between AA residues			Protein	Estimated distance between AA residues		
Protein	219 and 98	98 and 155	155 and 219		218 and 97	97 and 154	154 and 218		215 and 95	95 and 152	152 and 215
Ady2	4.6	6.9	4.0	Ato2	4.2	5.7	4.4	Ato3	4.0	4.6	4.1
Ady2 L219V	4.4	6.9	**5.3**	Ato2 L218S	**5.9**	5.6	**5.6**	Ato3 F95S	**7.7**	**8.5**	4.5
Ady2 A252G	4.5	6.7	3.9								

observed for any of the strains expressing Ato2, Ato3 or Ady2 variants. However, slow, non-exponential growth was observed for strains expressing *ATO2*^{T653C} or any variant of *ADY2* which could indicate a minor change in affinity for this substrate caused by the point mutations.

Protein modeling reveals mutations in the central hydrophobic constriction site as important factor in determining substrate specificity

In order to establish a link between the observed phenotypes and the structural alterations of transporters carrying the mutated amino acid residues, the 3D protein structures of Ady2, Ato2 and Ato3 were predicted based on the crystal structure of the *Citrobacter koseri* acetate anion channel SatP (PDB 5YS3), a bacterial member of the AceTr family (Qui *et al.* 2018). When combined with a sequence alignment of Ady2, Ato2 and Ato3, the 3D structures showed that the Leu219Val mutation in Ady2, the Leu218Ser mutation in Ato2 and the Phe95Ser mutation in Ato3 are amongst three amino acid residues that were previously identified to be essential for the formation of the central narrowest hydrophobic constriction of the anion pathway in *C. koseri* SatP (Qui *et al.* 2018; Figs 3 and 4). Specifically, these changes result in the substitution of the amino acid side group with a smaller (and in the case of Ato2 and Ato3 a more hydrophilic) alternative (Ato3 is shown in Fig. 4 and the models for Ady2 and Ato2 can be found in Figures S9 and S10, Supporting Information). Based on these models, we estimated the distance between these three hydrophobic residues. Since these distances are based on model predictions and are, for instance, dependent on the rotation of the amino acid side chains, they should not be interpreted as exact values. However, when comparing the relative distances, we found an increased value for *ADY2*^{C655G}, *ATO3*^{T284C} and *ATO2*^{T653C} compared to their corresponding wildtype protein, leading to a larger aperture in the center of the channel (Table 4). We hypothesize that this increased size of the hydrophobic constriction may allow larger substrates to pass through, possibly altering substrate specificity and transport capacity.

To investigate if the mutations affected the presence and affinity of binding sites for acetate, lactate and pyruvate, docking of ligands in the protein structures was simulated using AutoDock Vina (Figure S10 and Table S2, Supporting Information). In all proteins, both wildtype and mutated, four binding sites were identified for acetate, which is in accordance with what has previously been reported for the homolog CkSatP (Qui *et al.* 2018). Of these four binding sites, two, which are located closest to the hydrophobic constriction, also consistently bind lactate and pyruvate. Strikingly, mutations in Ady2, Ato2 and Ato3 led to an increased lactate affinity of at least one of these two sites closest to the hydrophobic constriction, which might have contributed to the increased lactate transport capacity. No clear correlation was found between the physiology observed for strains overexpressing the different protein variants when grown on acetate and pyruvate and the corresponding binding affinities of these two ligands (Table S2, Supporting Information).

DISCUSSION

In this study, we report the identification and characterization of a family of transporter genes which, upon mutation, are able to efficiently catalyze the import of lactic acid in *S. cerevisiae*. As rational engineering to identify lactic acid transporters remains elusive (Mans *et al.* 2017; Borodina 2019), we used adaptive laboratory evolution to select for mutants capable of consuming lactic acid, which led to the identification of mutations in *ATO3* (*ATO3*^{T284C}) and *ATO2* (*ATO2*^{T653C}). Together with *ADY2*, *ATO2* and *ATO3* were previously described to code for ammonium transporters (Ammonium Transport Outwards) based on two observations: the high expression levels of these genes when *S. cerevisiae* exports ammonium, and the presence of a motif associated with ammonium transport in the encoded proteins (Palková *et al.* 2002). However, the function of *ADY2* has previously been assessed by Rabitsch *et al.* (2001), who identified it as a gene required for correct spore formation, and thus named it as *ADY2* (Accumulation of DYads). In view of the observations in our study, where *ADY2*, *ATO2* and *ATO3* and their evolved variants catalyzed uptake of lactic and in some cases acetic acid, and the absence of mechanistic studies aimed at illustrating the phenomenon of ammonium export, we support the recent proposition by Alves *et al.* (2020) to rename these genes, present in *S. cerevisiae* and other yeasts, as 'Acetate Transporter Ortholog'.

For physiological studies focused on organic acid substrate uptake, a platform strain devoid of organic acid importers is a useful tool as it enables characterization based on growth rate. No growth was observed for IMC164 (25 deletions and empty vector) on medium containing either lactic acid or pyruvate as sole carbon source (Fig. 1), demonstrating that this is a suitable strain background to test pyruvic and lactic acid transport capacity of transporter variants. Strain IMK982 (*jen1Δ ady2Δ ato3Δ ato2Δ*) was also unable to grow on lactic acid, nor could it evolve this trait, which suggests that this strain could also be employed as a platform strain to investigate both endogenous and heterologous lactic acid transporters, without requiring the additional 21 deletions. In contrast, when grown on acetic acid at pH 6.0,

IMC164 exhibited non-exponential linear growth (Figure S6, Supporting Information), suggesting simple diffusion of acetic acid, or the presence of at least one gene involved in acetate transport in this strain background. The observed increase in the uptake rate of acetic acid for the evolved Ady2 and Ato2 variants (Fig. 2) corroborates with the increased growth rate on this carbon source. For the strain expressing native *ATO3* an improved growth rate was observed, but no increase in acetic acid uptake could be detected. This result led us to postulate the role of Ato3 as an exporter of acetic acid, thereby limiting the negative effects caused by the passive diffusion of this monocarboxylic acid. The fact that the expression of native *ATO3*, besides *ADY2*, results in an increased growth rate on acetate is in accordance with previous data reporting that both genes are induced in cells shifted from glucose to acetic acid as sole carbon source (Paiva *et al.* 2004).

It was reported by de Kok *et al.* (2012) that the overexpression of *ADY2*, under the control of the strong glycolytic promoter *TEF1*, was sufficient to enable slow growth (μ_{max} ~0.02 h^{-1}) in medium containing lactic acid as sole carbon source. While the native alleles of *ATO3* and likely *ATO2* were not able to sustain growth on lactic acid medium, their mutated versions (*ATO2*^{T653C} and *ATO3*^{T284C}) enabled high growth rates, with the highest growth rate determined at 0.15 ± 0.01 h^{-1} for the strain harboring *ATO3*^{T284C}. To the best of our knowledge this growth rate represents the highest reported growth rate of *S. cerevisiae* expressing a single transport protein on lactic acid and is close to the growth rate observed by de Kok *et al.* (2012) of 0.14 h^{-1} by a strain expressing *ADY2*^{C655G}. This 3-fold increase in growth rate of the engineered strain compared to the reference strain CEN.PK113-7D indicates that, in non-engineered *S. cerevisiae* strains, growth on lactic acid is likely limited by its transport into the cell, and not the capacity to be further metabolized. Therefore, for future work that requires fast consumption of lactic acid, overexpression of *ATO3*^{T284C} can be considered.

Based on the 3D structures of Ady2 (Ato1), Ato2 and Ato3 and the simulation of ligand docking in the predicted protein structures, we postulate that an increased binding affinity upon mutation may contribute to increased transport capacity by facilitating passage of the ligand through the hydrophobic constriction, although the increased size of the hydrophobic constriction is probably the main contributor to the evolved phenotype. Other mechanisms may also contribute to an improved transport capacity, as observed for the A252G mutation in Ady2, an amino acid residue located outside the constriction pore. These may include an improved transition between the closed to open state of the transporter or increased stability in the plasma membrane.

In this study, we show that laboratory evolution is a powerful tool for the identification of genes involved in substrate transport and resulted in the identification of Ato3^{F95S}, which enables the highest growth rate on lactic acid by *S. cerevisiae* reported in strains expressing a single transport protein thus far. In addition, the presented data on transporter structure and function led to the identification of important amino acid residues that dictate substrate specificity of *S. cerevisiae* carboxylic acid transporters, which could potentially aid in future rational engineering and annotation of additional proteins involved in organic acid transport.

SUPPLEMENTARY DATA

Supplementary data are available at FEMSYR online.

FUNDING

This work was supported by the BE-Basic R&D Program, which was granted an FES subsidy from the Dutch Ministry of Economic Affairs, Agriculture and Innovation (EL&I); the strategic programme UID/BIA/04050/2019 funded by Portuguese funds through the FCT I.P.; the projects: PTDC/BIAMIC/5184/2014, funded by national funds through the Fundação para a Ciência e Tecnologia (FCT) I.P.; the European Regional Development Fund (ERDF) through the COMPETE 2020–Programa Operacional Competitividade e Internacionalização (POCI); EcoAgriFood: Innovative green products and processes to promote AgriFood BioEconomy [grant number NORTE-01–0145-FEDER-000 009]; Norte Portugal Regional Operational Programme (NORTE 2020), under the PORTUGAL 2020 Partnership Agreement, through the European Regional Development Fund (ERDF); and UMINHO/BD/25/2016 PhD grant by the Norte2020 [grant number NORTE-08–5369-FSE-000 060] and a FEBS Short-Term Fellowship to MSS.

Conflicts of Interest. None declared.

REFERENCES

Agrimi G, Steiger MG. Metabolite transport and its impact on metabolic engineering approaches. *FEMS Microbiol Lett* 2021;**368**:fnaa211.

Alves R, Sousa-Silva M, Vieira D *et al.* Carboxylic acid transporters in *Candida* Pathogenesis. *mBio* 2020;**11**:e00156–20.

Anjos J, de Sousa HR, Roca C *et al.* Fsy1, the sole hexose-proton transporter characterized in *Saccharomyces yeasts*, exhibits a variable fructose:H^+ stoichiometry. *Biochimica et Biophysica Acta* 2013;**1828**:201–7.

Borodina I. Understanding metabolite transport gives an upper hand in strain development. *Microb Biotechnol* 2019;**12**:69–70.

Botstein D, Falco SC, Steward SE *et al.* Sterile Host Yeasts (SHY): a eukaryotic system of biological containment for recombinant DNA techniques. *Gene* 1979;**8**:17–24.

Bueno JGR, Borelli G, Corrêa TLR *et al.* Novel xylose transporter Cs4130 expands the sugar uptake repertoire in recombinant *Saccharomyces cerevisiae* strains at high xylose concentrations. *Biotechnol Biofuels* 2020;**13**. DOI: 10.1186/s13068-020-01782-0.

Casal M, Queirós O, Talaia G *et al.* Carboxylic acids plasma membrane transporters in saccharomyces cerevisiae. In: Ramos J, Sychrová H Kschischo M (eds.). *Yeast Membrane Transport*. Cham: Springer International Publishing, 2016, 229–51.

Casal M, Paiva S, Andrade RP *et al.* The lactate-proton symport of *Saccharomyces cerevisiae* is encoded by *JEN1*. *J Bacteriol* 1999;**181**:2620–3.

Chattopadhyay A, Singh R, Das AK *et al.* Characterization of two sugar transporters responsible for efficient xylose uptake in an oleaginous yeast *Candida tropicalis* SY005. *Arch Biochem Biophys* 2020;**695**:108645.

Cherry JM, Hong EL, Amundsen C *et al.* Saccharomyces genome database: the genomics resource of budding yeast. *Nucleic Acids Res* 2012;**40**:D700–5.

Colabardini AC, Ries LNA, Brown NA *et al.* Functional characterization of a xylose transporter in*Aspergillus nidulans*. *Biotechnol Biofuels* 2014;**7**:46.

de Kok S, Nijkamp JF, Oud B *et al.* Laboratory evolution of new lactate transporter genes in a*jen1*Δ mutant of *Saccharomyces cerevisiae* and their identification as *ADY2* alleles by whole-genome resequencing and transcriptome analysis. *FEMS Yeast Res* 2012;**12**:359–74.

Entian K-D, Kötter P. Yeast genetic strain and plasmid collections. *Front Microbiol* 2007;**36**:629–66.

Gabba M, Frallicciardi J, van 't Klooster J *et al.* Weak acid permeation in synthetic lipid vesicles and across the yeast plasma membrane. *Biophys J* 2020;**118**:422–34.

Gao M, Ploessl D, Shao Z. Enhancing the co-utilization of biomass-derived mixed sugars by yeasts. *Front Microbiol* 2019;**9**:3264.

Gietz RD, Woods RA. Transformation of yeast by lithium acetate/single-stranded carrier DNA/Polyethylene glycol method. *Methods Enzymol* 2002;**350**:87–96.

Huang W, Hu B, Liu J *et al.* Identification and characterization of Tonoplast Sugar Transporter (TST) gene family in cucumber. *Hortic Plant J* 2020;**6**:145–57.

Kruckeberg AL, Dickinson JR. Carbon metabolism. In: Dickinson JR, Schweizer M (eds.). *The Metabolism and Molecular Physiology of Saccharomyces cerevisiae*. London: Taylor & Francis Ltd, 2004, 42–103.

Lagunas R. Sugar transport in *Saccharomyces cerevisiae*. *FEMS Microbiol Lett* 1993;**104**:229–42.

Li H, Durbin R. Fast and accurate long-read alignment with Burrows–Wheeler transform. *Bioinformatics* 2010;**26**:589–95.

Li H, Handsaker B, Wysoker A *et al.* The sequence alignment/map format and SAMtools. *Bioinformatics* 2009;**25**:2078–9.

Li H, Schmitz O, Alper HS. Enabling glucose/xylose co-transport in yeast through the directed evolution of a sugar transporter. *Appl Microbiol Biotechnol* 2016;**100**:10215–23.

Li J, Xu J, Cai P *et al.* Functional analysis of two L-arabinose transporters from filamentous fungi reveals promising characteristics for improved pentose utilization in *Saccharomyces cerevisiae*. *Appl Environ Microbiol* 2015;**81**:4062–70.

Lõoke M, Kristjuhan K, Kristjuhan A. Extraction of genomic DNA from yeasts for PCR-based applications. *BioTechniques* 2011;**50**:325–8.

Mans R, Daran J-MG, Pronk JT. Under pressure: evolutionary engineering of yeast strains for improved performance in fuels and chemicals production. *Curr Opin Biotechnol* 2018;**50**:47–56.

Mans R, Hassing J-E, Wijsman M *et al.* A CRISPR/Cas9-based exploration into the elusive mechanism for lactate export in *Saccharomyces cerevisiae*. *FEMS Yeast Res* 2017;**17**:1–12.

Mans R, van Rossum HM, Wijsman M *et al.* CRISPR/Cas9: a molecular Swiss army knife for simulaneous introduction of multiple genetic modifications in *Saccharomyces cerevisiae*. *FEMS Yeast Res* 2015;**15**:1–15.

Marques WL, Mans R , Marella RE *et al.* Elimination of sucrose transport and hydrolysis in *Saccharomyces cerevisiae*: a platform strain for engineering sucrose metabolism. *FEMS Yeast Research* 2017;**17**:1–11.

Morii M, Sugihara A, Takehara S *et al.* The dual function of OsSWEET3a as a gibberellin and glucose transporter is important for young shoot development in rice. *Plant Cell Physiol* 2020;**61**:1935–45.

Mumberg D, Müller R, Funk M. Yeast vectors for the controlled expression of heterologous proteins in different genetic backgrounds. *Gene* 1995;**156**:119–22.

Nijland JG, Driessen AJM. Engineering of pentose transport in *Saccharomyces cerevisiae* for biotechnological applications. *Front Bioeng Biotechnol* 2020;**7**:464.

Nogueira KMV, Mendes V, Carraro CB *et al.* Sugar transporters from industrial fungi: key to improving second-generation ethanol production. *Renew Sustain Energy Rev* 2020;**131**:109991.

Paiva S, Devaux F, Barbosa S *et al.* Ady2p is essential for the acetate permease activity in the yeast *Saccharomyces cerevisiae*. *Yeast* 2004;**21**:201–10.

Palková Z, Devaux F, Řičicová M *et al.* Ammonia pulses and metabolic oscillations guide yeast colony development. *Mol Biol Cell* 2002;**13**:3901–14.

Paulsen PA, Custódio TF, Pedersen BP. Crystal structure of the plant symporter STP10 illuminates sugar uptake mechanism in monosaccharide transporter superfamily. *Nat Commun* 2019;**10**. DOI: 10.1038/s41467-018-08176-9.

Pinheiro C, Longatto-Filho A, Azevedo-Silva J *et al.* Role of monocarboxylate transporters in human cancers: state of the art. *J Bioenerg Biomembr* 2012;**44**:127–39.

Pronk JT. Auxotrophic yeast strains in fundamental and applied research. *Appl Environ Microbiol* 2002;**68**:2095–100.

Qui B, Xia B, Zhou Q *et al.* Succinate-acetate permease from *Citrobacter koseri* is an anion channel that unidirectionally translocates acetate. *Cell Res* 2018;**28**:644–54.

Rabitsch KP, Tóth A, Gálová M *et al.* A screen for genes required for meiosis and spore formation based on whole-genome expression. *Curr Biol* 2001;**11**:1001–9.

Ribas D, Sá-Pessoa J, Soarez-Silva I *et al.* Yeast as a tool to express sugar acid transporters with biotechnological interest. *FEMS Yeast Res* 2017;**17**. DOI: 10.1093/femsyr/fox005.

Ribas D, Soares-Silva I, Vieira D *et al.* The acetate uptake transporter family motif "NPAPLGL(M/S)" is essential for substrate uptake. *Fungal Genet Biol* 2019;**122**:1–10.

Riesmeier JW, Willmitzer L, Frommer WB. Isolation and characterization of a sucrose carrier cDNA from spinach by functional expression in yeast. *EMBO J* 1992;**11**:4705–13.

Salazar AN, Gorter de Vries AR, van den Broek M *et al.* Nanopore sequencing enables near-complete de novo assembly of*Saccharomyces cerevisiae* reference strain CEN.PK113-7D. *FEMS Yeast Res* 2017;**17**:1–11.

Schmidl S, Iancu CV, Reifenrath M *et al.* A label-free real-time method for measuring glucose uptake kinetics in yeast. *FEMS Yeast Res* 2021;**21**:foaa069.

Singhvi M, Zendo T, Sonomoto K. Free lactic acid production under acidic conditions by lactic acid bacteria strains: challenges and future prospects. *Appl Microbiol Biotechnol* 2018;**102**:5911–24.

Sloothaak J, Tamayo–Ramos JA, Odoni DI *et al.* Identification and functional characterization of novel xylose transporters from the cell factories *Aspergillus niger* and *Trichoderma reesei*. *Biotechnol Biofuels* 2016;**9**:148.

Soares-Silva I, Ribas D, Sousa-Silva M *et al.* Membrane transporters in the bioproduction of organic acids: state of the art and future perspectives for industrial applications. *FEMS Microbiol Lett* 2020;**367**:fnaa118.

Sterling T, Irwin JJ. ZINC 15 – ligand discovery for everyone. *J Chem Inf Model* 2015;**55**:2324–37.

Suzuki Y, St Onge RP, Mani R *et al.* Knocking out multigene redundancies via cycles of sexual assortment and fluorescence selection. *Nat Methods* 2011;**8**:159–64.

Trott O, Olson AJ. AutoDock Vina: improving the speed and accuracy of docking with a new scoring function, efficient optimization, and multithreading. *J Comput Chem* 2010;**31**:455–61.

Verduyn C, Postma E, Scheffers WA *et al.* Effect of benzoic acid on metabolic fluxes in yeasts: a continuous-culture study on the regulation of respiration and alcoholic fermentation. *Yeast* 1992;**8**:501–17.

Walker BJ, Abeel T, Shea T *et al*. Pilon: an integrated tool for comprehensive microbial variant detection and genome assembly improvement. *PLoS One* 2014;**9**:e112963.

Wang C, Shen Y, Hou J *et al*. An assay for functional xylose transporters in *Saccharomyces cerevisiae*. *Anal Biochem* 2013;**442**:241–8.

Wieczorke R, Krampe S, Weierstall T *et al*. Concurrent knock-out of at least 20 transporter genes is required to block uptake of hexoses in *Saccharomyces cerevisiae*. *FEBS Lett* 1999;**464**:123–8.

Zhang W, Cao Y, Gong J *et al*. Identification of residues important for substrate uptake in a glucose transporter from the filamentous fungus *Trichoderma reesei*. *Sci Rep* 2015;**5**:13829.